

Effects of doping on the dynamic mechanical response of semiconductor cantilevers to electrostatic forces

Albert K. Henning

Thayer School of Engineering, Dartmouth College, Hanover NH 03755-8000

ABSTRACT

The theory of electrostatic forces on doped semiconductor cantilevers, and their dynamic, mechanical response, is presented. Effects of constant, and time-varying, voltages between the cantilever and a mechanically fixed reference potential are studied. Surface charges are considered, since they can screen electrostatic forces significantly.

The results show work function differences between the cantilever and the reference electrode must be included in calculating the mechanical response of semiconductor cantilevers to electrostatic forces. Surface charges, as long as their sheet densities are below 10^{11} cm⁻², will not present especial difficulties for either analysis or behavior. Small-signal analysis of the mechanical response is complicated by both large-signal applied biases, giving rise to displacement currents, and penetration of the electric field into non-degenerate semiconductors.

Keywords: microcantilever; atomic force microscope; AFM; electrostatic force microscope; EFM; semiconductor cantilever; scanning Kelvin probe microscope; SKPM; dopant profile; dynamic response; cantilever mechanical transfer function; small signal.

1. INTRODUCTION

Micro-fabricated cantilevers have two primary industrial applications. Scanning force microscopes frequently utilize silicon cantilevers as their sensor elements¹. Atomic force measurements then allow extraction of surface topography², while electrostatic force measurements allow determination of semiconductor dopant profiles^{3,4}, and sub-surface charge densities in microelectronic circuits⁴. Similarly, micro-accelerometers such as Analog Devices' ADXL50 utilize a tethered, surface micro-machined, polysilicon cantilever⁵. Mechanical motion of this cantilever is sensed capacitively, leading to an accurate and reliable sensor for airbag deployment in automobiles.

Cantilevers also appear in fundamental research related to the properties of micro-fabricated structures. Linear comb drives and other resonant microstructures have been studied⁶. The bending of in-plane⁷ and out-of-plane⁸ polysilicon cantilevers after mechanical release using hydrofluoric acid (HF) is of considerable interest. Fixed-free and fixed-fixed cantilevers have been used to extract mechanical properties of polysilicon, such as Young's modulus⁹. Most recently, the problems of the force on a point charge near a semiconductor surface¹⁰, and the electrostatic force between a metallic tip and a semiconductor surface¹¹ have been explored.

In most of these cases, since the cantilever is constructed of doped silicon, the electrostatic force on the cantilever differs from that found in purely metallic cantilevers. First, the polarity of the dopant (n- or p-type) can add a work function difference between the cantilever and the source or termination of electric field lines, altering the electrostatic force on the cantilever. Second, if the cantilever is not degenerately doped, the field lines can penetrate the semiconductor significantly, again altering the electrostatic force.

In this work, the effects of work function differences between a cantilever and a substrate, and penetration of lines of electric force into a semiconductor cantilever electrode, are studied. The theory leading to the equations of motion of the cantilever are presented. Thereafter, case studies for a variety of metal and semiconductor systems are described. Finally, the effects of surface charge, and of displacement currents generated by the moving cantilever, are considered.

2. THEORY

2.1 System description

Figure 1 shows a schematic representation of the micro-cantilever system under study. Figure 1a shows the schematic for an atomic force microscope (AFM) or electrostatic force microscope (EFM). This structure represents the most general electromechanical case which might be studied. It receives two inputs, which vary sinusoidally at different frequencies. The first input is a mechanical force $f(t)$, due to the oscillations in the piezoelectric stack which can excite various normal modes in the distributed mass of the cantilever. The second input is an electrochemical potential difference (EPD) $U(t)$, due to the voltage applied between the cantilever and the substrate.

Figure 1b simplifies the structure of Figure 1a. The cantilever is shown to be anchored or fixed at one end, and free to move at the other. The actuation or sensing due to $U(t)$ is effected through the electrostatic coupling between the cantilever and the substrate. The electrostatic force is taken to act only at the end of the cantilever, and is represented in the figure as a capacitor with variable separation between plates. The substrate is taken to be a metal, or a semiconductor which may or may not be degenerately doped. For purposes of expressing spring constants and resonant frequencies, the cantilever has a length L , a width W , and a thickness H . It is taken to be a metal, though it may also be a semiconductor (see Section 4.3). The actual effects of atomic forces (e.g. due to Lennard-Jones potential gradients) are neglected in this analysis.

A lumped element approach will be taken for analysis, shown in Figure 1c. The mass M represents the lumped mass of the cantilever, including any extra mass at the free end due to a tip. The spring constant K considers only the lowest order normal mode of vibration of the cantilever. The frictional forces are lumped into a single parameter B . Quality factors which set the damping coefficient vary, but a value of $Q=100$ is not atypical. The mechanical input $f(t)$, and the electrical input $U(t)$, remain. The separation between the mass and the substrate is $x(t)$.

The task, then, is to determine the electrostatic potential $\psi(z,t)$, and the separation of the mass and substrate $x(t)$.

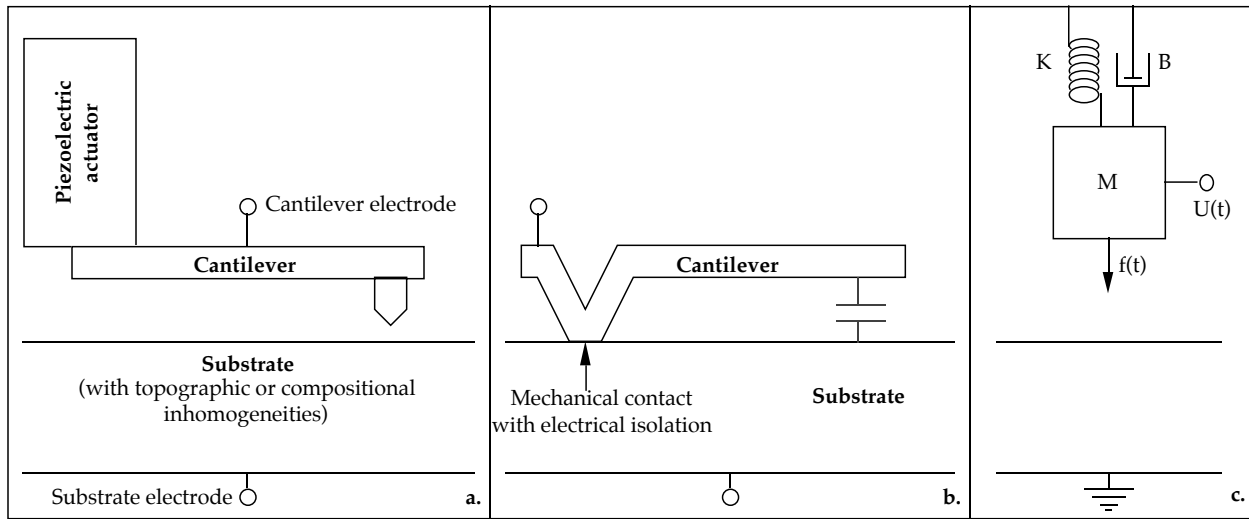


Figure 1: a. Schematic of AFM cantilever; b. Schematic of ideal cantilever studied in this work; c. One-dimensional system model of the cantilever studied in this work

2.2 Energy band considerations

In order to accomplish this task, we must consider the energy band diagram associated with the cantilever-substrate system. We confine ourselves to a one-dimensional treatment of the energy bands. Some of the effects of three dimensions have been considered elsewhere¹¹. Save for the mechanical motion, the situation mirrors the common metal-insulator-semiconductor device which lies at the heart of modern microelectronics¹². This addition, however, creates important differences from that device.

Consider Figure 2 in this light. The electrically conductive cantilever (which could itself be a metal, or a non-degenerately or degenerately doped semiconductor) is on the left. It has a work function ϕ_m , and an EPD $U(t)$ relative to the (assumed to be grounded) substrate. The substrate may have a different work function than the cantilever. If it is a semiconductor, the substrate's doping sets its work function ϕ_s . The band bending ψ_s in the semiconductor is a result of material factors such as doping and dielectric constant, as well as electrical boundary conditions such as $U(t)$, and mechanical boundary conditions $x(t)$. V_{ins} is the band bending in the insulator separating the cantilever and the substrate. The insulator most typically will be air, and less frequently water.

SKPM techniques rely heavily on this band picture⁴. In that technique, the electrostatic force is minimized. This minimization creates a null in the mechanical oscillation of the cantilever. In effect the flatband voltage (V_{FB}) is applied between the cantilever and substrate, in order to minimize the mechanical vibration. However, the EPD is *not* minimized. It is crucial therefore to realize that electrostatic potential and electrochemical potential are not the same.

The substrate as shown is doped p-type. However, the substrate may be doped n- or p-type. The doping may be inhomogeneous. Also, the band bending in the substrate will fall into one of four categories: *accumulation*; *depletion*; *flatband* (where the electrostatic force is zeroed); and *inversion*. Figure 2 depicts a depletion state.

Note that 'substrate' can also be taken to mean the fixed electrode in a system with a movable cantilever. This extension of meaning allows the treatment here to describe lateral resonant structures, and not simply structures with motion perpendicular to a monolithic, large area substrate.

Note that in this energy band diagram, positive (electron) voltage is in the direction of negative energy. And, given the discontinuities in the conduction band, the proper electrostatic potential reference is the vacuum level.

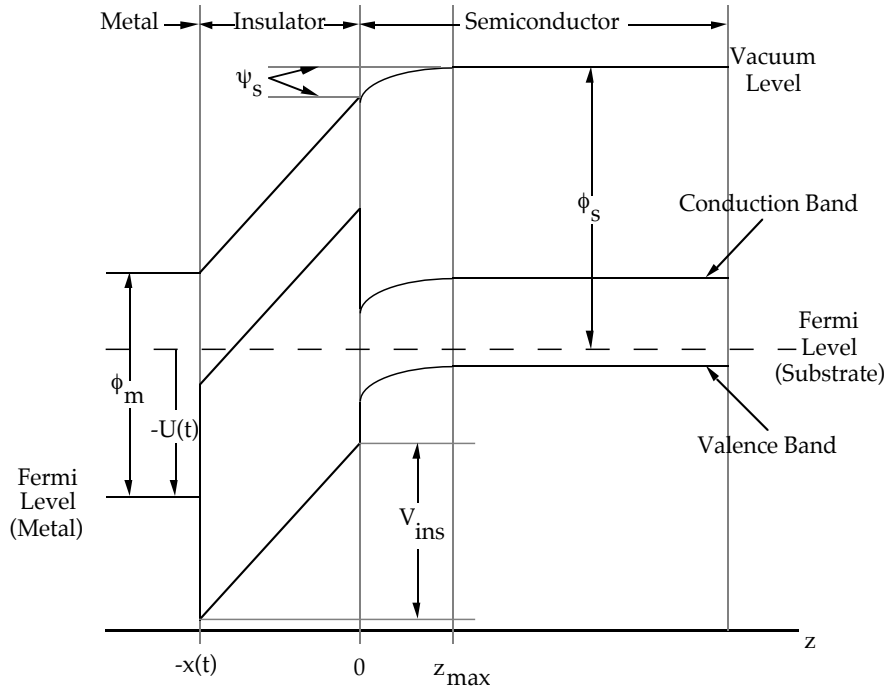


Figure 2: One-dimensional energy band diagrams used in this work.

2.3 Derivation of equations of motion

The equations of motion for the system shown in Figure 1c become, using a state variable representation:

$$\frac{dv}{dt} = \frac{1}{M} \{ f(t) - B v - K x - M g + F_e \}$$

$$\frac{dx}{dt} = v \quad (1)$$

$x(t)$ and $v(t)$ are the state variables of the system, describing the position and velocity of the cantilever mass relative to the substrate. The system inputs are $f(t)$, the external mechanical force (which in the case of an AFM cantilever is applied using a piezoelectric transducer), and $U(t)$, the EPD (which will be evident in a moment). The mass M is given by $\rho L W H$, where ρ is the mass density of the cantilever material. B is the damping coefficient. The spring constant for the fundamental normal mode of a cantilever fixed at one end only is given by^{12a}:

$$K = 4.11 \frac{W H}{L} E \quad (2)$$

E is the Young's modulus for the cantilever material. Note that W/L is the number of squares in a plan view of the cantilever atop the substrate, making K related to the material property E and the film thickness H parallel to the direction of cantilever oscillation. g is the gravitational acceleration; oscillations in the plane perpendicular to the gravitational force allow neglect of this term.

F_e is the electrostatic force between the cantilever and the substrate. (F_e is given below in force per unit area, consistent with the definitions of electrostatic charge and energy; other factors in the equation of motion are not per unit area.) It is a function of the separation between the cantilever and the substrate. It is also a function of the EPD $U(t)$ applied between the cantilever and the substrate. This force is affected fundamentally by electric field penetration into either the cantilever or the tip. Following Figure 2, the total potential drop from the cantilever to the substrate is broken into V_{ins} (the drop in the insulator), and ψ_s (the drop in the semiconductor). If the cantilever is a semiconductor, then there is an additional drop there. If the semiconductor surface has charges, then there is a discontinuity in the electric field at the surface due to this charge.

A related analysis for F_e has been given elsewhere recently¹¹. That treatment neglected two crucial aspects. First, it did not incorporate surface charges. Second, it presumed that both the electrical response to $U(t)$ and the mechanical response $x(t)$ were *small-signal* quantities. This assumption is usually wrong for AFM cantilevers, and frequently (but not always) incorrect for cantilevers such as those found in microaccelerometers. For these reasons, we make a more complete derivation here, where the inclusion of Equation 1 does not limit us to small-signal analysis. We also note, but do not treat here except through a later discussion of displacement current, that redistribution of charges along the length of a distributed (not lumped) cantilever can have important ramifications for its dynamic behavior¹³.

To find F_e , we begin with the energy contained in the electric field in the cantilever-substrate system. The electrostatic energy per unit area is:

$$w = \frac{W}{A} = \frac{1}{2A_{vol}} \int \mathbf{D} \cdot \mathbf{E} \, dv = \frac{1}{2} \int \mathbf{D} \cdot \mathbf{E} \, dz \quad (3)$$

Our challenge is to find the displacement D and electric field E at every point in the calculation volume. This task can be accomplished using Gauss's Law, and the appropriate boundary conditions. There are three of these. At $z=-x(t)$, the boundary condition on ψ is:

$$\psi [-x(t), t] = \phi_m - U(t) \quad (4)$$

The negative sign on the EPD $U(t)$ ensures that positive biases on the cantilever will pull the bands on the left of Figure 2 *down* in (electron) energy. At $z=z_{max}$ we have:

$$\psi (z_{\max}) = \phi_s \quad (5)$$

At $z=0$, Gauss's Law and the continuity of the displacement D ensure the third relevant boundary condition:

$$\epsilon_s E (0^+) - \epsilon_{\text{ins}} E (0^-) = \epsilon_s E_s - \epsilon_{\text{ins}} E_{\text{ins}} = q N_f \quad (6)$$

ϵ_s and ϵ_{ins} are the dielectric constants of the semiconductor and insulator, respectively. E_s is the electric field in the surface of the semiconductor. E_{ins} is the electric field in the insulator, whose magnitude is given by $V_{\text{ins}}/x(t)$ if there are no fixed charges in this region. N_f is the surface charge number density (per unit area) on the semiconductor.

If the substrate is a semiconductor, we must solve Poisson's equation in order to determine $\psi(z,t)$. We write this equation as:

$$\epsilon_s \frac{dE}{dz} = -\epsilon_s \frac{d^2\psi}{dz^2} = q [p_0 \exp (-\beta\psi) - n_0 \exp (\beta\psi) - N_a] \quad (7)$$

The electric field $E=-d\psi/dz$, $n_0 p_0 = n_i^2$, and $\beta=q/kT$, where n_i is the intrinsic carrier concentration in the semiconductor, k is Boltzmann's constant and T is the lattice temperature. N_a is the dopant concentration in the substrate, which is assumed to be p-type and distributed uniformly. n_0 and p_0 are the electron and hole carrier concentrations beyond the semiconductor band-bending. This expression can be integrated once analytically to obtain the electric field:

$$E (\psi) = E_0 \sqrt{ \exp (-\beta\psi) + \beta\psi - 1 + \frac{n_0}{p_0} [\exp (\beta\psi) - \beta\psi - 1] } \quad (8)$$

where $E_0 = (q p_0 / \beta \epsilon_s)$. Note that the surface electric field can be found using Equation 8, such that $E_s = E(\psi_s) \text{sgn}(\psi_s)$. The expression which links ψ_s with the various inputs and material parameters of the system can be found by inspection of Figure 2, and using Equation 6:

$$\begin{aligned} U(t) + \phi_s &= \phi_m + V_{\text{ins}} + \psi_s \\ \therefore U(t) &= \phi_{\text{ms}} + \frac{x(t)}{\epsilon_{\text{ins}}} [\epsilon_s E_s - q N_f] + \psi_s \\ \therefore U(t) &= V_{\text{FB}} + \psi_s + \frac{x(t)}{\epsilon_{\text{ins}}} \epsilon_s E_s \end{aligned} \quad (9)$$

This expression can be understood physically as the equation of two terms: the applied EPD in excess of the flatband; and the sum of the band bendings in the semiconductor and insulator. Note that, for a given $x(t)$ and $U(t)$, Equations 8 and 9 allow determination of a unique value of surface potential ψ_a . Note also the implicit definition for the flatband voltage V_{FB} in Equation 9, which includes the surface charge N_f .

We can now find the electrostatic energy by evaluating explicitly the integral in Equation 3:

$$w = \frac{1}{2} \int_{-x(t)}^{z_{\max}} D \cdot E \, dz = \frac{1}{2} \left\{ \int_{-x(t)}^0 \epsilon_{\text{ins}} E_{\text{ins}}^2 \, dz + \int_0^{z_{\max}} \epsilon_s E^2(z) \, dz \right\} \quad (10)$$

The first integral is determined easily, again using Equation 6:

$$\frac{1}{2} \epsilon_{\text{ins}} E_{\text{ins}}^2 x(t) = \frac{x(t)}{2 \epsilon_{\text{ins}}} [\epsilon_s^2 E_s^2 - 2 q \epsilon_s N_f E_s + q^2 N_f^2] \quad (11)$$

The second integral can also be determined by using the definition of the electric field as the negative gradient of the electrostatic potential, and changing variables from z to ψ . This procedure yields an integral which is fairly simple to evaluate numerically:

$$\int_0^{z_{\text{max}}} \epsilon_s E^2(z) dz = \frac{1}{2} \int_0^{\psi_s} d\psi \operatorname{sgn}(\psi_s) \epsilon_s E_0 \sqrt{\exp(-\beta\psi) + \beta\psi - 1 + \frac{n_0}{p_0} [\exp(\beta\psi) - \beta\psi - 1]} \quad (12)$$

The electrostatic force F_e is then found from the gradient of the electrostatic energy w with respect to the separation between the cantilever and the substrate $x(t)$:

$$F_e = \frac{dw}{dx} \quad (13)$$

The procedure is now specified completely. At a given time t , the inputs $f(t)$ and $U(t)$, and the initial conditions on $v(t)$ and $x(t)$, are known. Using $U(t)$ and $x(t)$, Equations 8 and 9 allow determination of ψ_s . Equation 13 then allows determination of the electrostatic force. Equation 1 then allows the state variables to be updated using either an Euler or Runge-Kutta method. The cycle of calculation repeats.

An alternative means to calculate the electrostatic force term required by the equations of motion is intriguing and attractive. If there are both surface and bulk charges in the semiconductor, then the electrostatic force will have components due to the bulk and the surface charges, $F_e = F_{\text{bulk}} + F_{\text{surface}}$. The force due to the bulk charges can be found by integrating the differential force $dF = E dq$ over the semiconductor substrate, where the charge per area $dq = \rho(z) dz$:

$$\begin{aligned} F_{\text{bulk}} &= \int_0^{z_{\text{max}}} \rho(z) E(z) dz = \int_{\psi_s}^0 \rho(\psi) E(\psi) \frac{dz}{d\psi} d\psi = \int_0^{\psi_s} \rho(\psi) d\psi \\ &= \int_0^{\psi_s} q \{ p_0 [\exp(-\beta\psi) - 1] - n_0 [\exp(\beta\psi) - 1] \} d\psi \\ &= q \{ (n_0 - p_0) \psi_s + \frac{p_0}{\beta} [1 - \exp(-\beta\psi_s)] + \frac{n_0}{\beta} [1 - \exp(\beta\psi_s)] \} \\ \therefore F_{\text{bulk}} &= -\epsilon_s E^2(\psi_s) = -\epsilon_s E_s^2 = -Q_s E_s \end{aligned} \quad (14)$$

Due to the configuration of the applied bias $U(t)$, this force is always attractive, so that for use in Equation 1, $F_{\text{bulk}} = \epsilon_s E_s^2$. The surface charge N_f will contribute to the force as well. This force can be determined by differentiating Equation 11 with respect to $x(t)$:

$$\begin{aligned} F_{\text{surface}} &= \frac{1}{2\epsilon_{\text{ins}}} [\epsilon_s^2 E_s^2 - 2 q \epsilon_s N_f E_s + q^2 N_f^2] \\ \therefore F_e(\psi_s) &= \epsilon_s E_s^2 \left(1 + \frac{\epsilon_s}{2\epsilon_{\text{ins}}} \right) - q N_f \frac{\epsilon_s}{\epsilon_{\text{ins}}} E_s + \frac{q^2 N_f^2}{2\epsilon_{\text{ins}}} \end{aligned} \quad (15)$$

The effect of the fixed surface charge will be to enhance (attraction) or diminish (repulsion) the force, depending upon the signs of N_f and $U(t)$, and the effect of $U(t)$ on E_s .

3. CASES

This procedure improves on previous work, by allowing large-signal analysis to be undertaken, and by considering the effects of surface charge. We now use this mathematical formulation to consider several cases of interest.

3.1 Mechanically fixed cantilever: Metal-metal system

This case is identical to the metal-insulator-metal capacitor, where the capacitor plates are fixed, and a solid insulator (say, SiO_2) fills the space between the capacitor plates. In this case, there is no band bending or electric field in the substrate metal, or in the 'cantilever'. Furthermore, there is no mechanical motion of the capacitor plates. As a result, Equation 9 gives the dynamic behavior of the system:

$$U(t) = \phi_{ms} - \frac{qN_f(t)}{C'_{ins}} \quad (16)$$

C'_{ins} is the capacitance per unit area of the system. The charge N_f becomes a function of time, in the usual relation of a capacitor's charge to the voltage applied to its plates. However, the work function difference between the plates is an important, and usually ignored, factor. N_f is a negative value for positive $U(t)$: it represents the negative charge which balances the positive charge on the $U(t)$ electrode. Note that a pressure does exist on the plates and the solid insulator, which can be determined from Equations 9 and 15. (F_e is in fact a pressure, since its units are force per unit area. This pressure may be considerable.)

3.2 Mechanically fixed cantilever: Metal-semiconductor system

This case is identical to the metal-oxide-semiconductor capacitor, where the capacitor plates are fixed. Equations 8 and 9 determine the dynamic behavior:

$$U(t) = V_{FB} + \psi_s(t) + \frac{\epsilon_s E_s [\psi_s(t)]}{C'_{ins}} \quad (17)$$

Here, the fixed surface charge is a constant of time, and appears in the flatband voltage only. The time dependent charge on the capacitor is represented by the numerator of the last term of this expression.

3.3 Mechanically free cantilever: Metal-metal system

This case corresponds to the vibration of a metal cantilever over a metal substrate, where the metals have different work functions. Using Equations 1, 9, and 15, and again remembering that $\psi_s = E_s = 0$:

$$\begin{aligned} \frac{dv}{dt} &= \frac{1}{M} \left\{ f(t) - Bv - Kx - Mg + \frac{q\epsilon_{ins}}{2x^2} [\phi_{ms} - U(t)]^2 \right\} \\ \frac{dx}{dt} &= v \end{aligned} \quad (18)$$

The inputs to the system are $U(t)$ and $f(t)$. The direct outputs are $x(t)$ and $v(t)$, though $N_f(t)$ is related to F_e , and therefore calculable. The electrostatic force has the familiar $1/x^2$ dependence. Again, however, the work function difference plays an important role in the response of the system.

3.4 Mechanically free cantilever: Metal-semiconductor system

This is the most general case. The full response of the system is given by Equations 1, 8, 9, and 15:

$$\frac{dv}{dt} = \frac{1}{M} \{ f(t) - Bv - Kx - Mg + F_e[\psi_s(t)] \}$$

$$\frac{dx}{dt} = v$$

$$F_e[\psi_s(t)] = \epsilon_s E_s[\psi_s(t)]^2 \left(1 + \frac{\epsilon_s}{2\epsilon_{ins}} \right) - qN_f \frac{\epsilon_s}{\epsilon_{ins}} E_s[\psi_s(t)] + \frac{q^2 N_f^2}{2\epsilon_{ins}}$$

$$E_s[\psi_s(t)] = E_0 \sqrt{\exp(-\beta\psi_s) + \beta\psi_s - 1 + \frac{n_0}{p_0} [\exp(\beta\psi_s) - \beta\psi_s - 1]}$$

$$U(t) = V_{FB} + \psi_s(t) + \frac{x}{\epsilon_{ins}} \epsilon_s E_s[\psi_s(t)]$$

Note that the gravitational component to the equation of motion need not be invoked for laterally resonant systems.

4. OTHER EFFECTS

4.1 Surface charge

For metal-metal systems, surface charge is a time-dependent variable, whereas in metal-semiconductor systems it is taken to be fixed. We can assess the impact of surface charges in a straightforward way. Consider the flatband voltage, and remember that in an electromechanical system it corresponds to the state of zero electrostatic force. Shifts in the flatband voltage are given by:

$$\Delta V_{FB} = \frac{q N_f \epsilon_{ins}}{x(t)} \quad (19)$$

This expression leads to two conclusions. First, even small amounts of fixed charge can, if the capacitor plate separation is small enough, lead to large changes in flatband voltage, and therefore large effects on the response and analysis of the system. Second, if a cantilever experiences large displacements relative to the substrate, again large changes in flatband voltage will occur.

4.2 Displacement current

Recently, studies of non-contact AFM systems have shown displacement currents to be important possible sources of error in analysis and interpretation of results¹⁴. The displacement current is given by:

$$I_{avg} = \lim_{T \rightarrow \infty} \frac{1}{T} \int_0^T \frac{\delta(CV)}{\delta t} d\tau \quad (20)$$

In an AFM cantilever, this current has been measured in the picoamp range, for mechanical oscillation frequencies of the forcing function $f(t)$ up to 200 kHz. This displacement current increases as the magnitude of the ac component of the electrical forcing function $U(t)$ increases.

4.3 Semiconductor-semiconductor systems

AFM tips are frequently comprised of semiconducting materials⁴. In this case, electric field lines will penetrate both the AFM tip and the substrate. Significant field penetration into the tip will spread the spatial extent of the semiconductor surface probed by the tip, thereby losing spatial resolution of the scanning probe measurement. Even so, while the analysis above will be quantitatively different, qualitatively little will change.

5. CONCLUSIONS

The effects of electrostatic forces on micro-fabricated cantilevers treated as capacitor plates with different work functions, and where one of the capacitor plates may be a semiconductor, have been presented. The effects of work function differences between the cantilever and substrate plates, and fixed charge on semiconductor surfaces, have been incorporated. The analysis makes no small-signal assumptions for either mechanical motion or applied bias, and therefore is most general. The analysis has been limited to a study of a lumped element model for the fundamental mode of oscillation of a vibrating cantilever, though higher order modes may be incorporated. The dynamic responses for mechanically fixed and mechanically free systems have been presented, for both metal-metal and metal-semiconductor electrostatic coupling.

6. ACKNOWLEDGEMENTS

The author acknowledges gratefully discussions with Charles P. Daghljan, Todd Hochwitz, Christopher G. Levey, and James A. Slinkman.

7. REFERENCES

1. R.C. Barrett and C.F. Quate, "Imaging polished sapphire with atomic force microscopy." *J. Vac. Sci. Tech.* **A8**, pp. 400-402 (1990).
2. G. Binnig, C. Gerber, E. Stoll, T.R. Albrecht, and C.F. Quate, "Atomic resolution with atomic force microscope." *Surf. Sci.* **189-190**, pp. 1-6 (1987).
3. Y. Huang, J. Slinkman, and C.C. Williams, "Modelling of impurity dopant density measurement in semiconductors by scanning force microscopy." *Ultramicroscopy* **42-44**, pt. A, pp. 298-303 (1991).
4. A.K. Henning, T. Hochwitz, J. Slinkman, J. Never, S. Hoffman, P. Kaszuba, and C.P. Daghljan, "Two-dimensional surface dopant profiling in silicon using scanning Kelvin probe microscopy." *J. Appl. Phys.* **77**, pp. 1888-1896 (1995).
5. T.A. Core, W.K. Tsang, and S.J. Sherman, "Fabrication technology for an integrated surface-micromachined sensor." *Sol. St. Tech.* **36**, pp. 39-40 (1993).
6. W.C. Tang, T.-C.H. Nguyen, M.W. Judy, and R.T. Howe, "Electrostatic-comb drive of lateral polysilicon resonators." *Sens. and Act.* **A21**, pp. 328-331 (1990).
7. M.W. Judy, Y.-H. Cho, R.T. Howe and A.P. Pisano, "Self-adjusting microstructures (SAMS)." in *Proc. IEEE Micro Electro Mech. Syst.* (IEEE, New York, 1991), pp. 51-56.
8. C.-L. Tsai and A.K. Henning, "Out-of-plane microstructures using stress engineering of thin films." in *SPIE Proc. Vol. 2639, Micromach. and Microfab. Proc. Tech.* (SPIE, Bellingham, WA, 1995).
9. P.M. Osterberg, *Electrostatically Actuated Microelectromechanical Test Structures for Material Property Measurement*. Ph.D. dissertation (Massachusetts Institute of Technology, Cambridge, MA, 1995).
10. C. Donolato, "Electrostatic problem of a point charge in the presence of a semi-infinite semiconductor." *J. Appl. Phys.* **78**, pp. 684-690 (1995).
11. S. Hudlet, M. Saint Jean, B. Roulet, J. Berger, and C. Guthmann, "Electrostatic forces between metallic tip and semiconductor surfaces." *J. Appl. Phys.* **77**, pp. 3308-3314 (1995).
12. E.H. Nicollian and J.R. Brews. *MOS (Metal Oxide Semiconductor) Physics and Technology* (John Wiley & Sons, New York, 1982).
- 12a. D. Sarid, *Scanning Force Microscopy with Applications to Electric, Magnetic, and Atomic Forces*. (Oxford University Press, New York, 1991).
13. P. Osterberg, H. Yie, X. Cai, J. White, and S. Senturia, "Self-consistent simulation and modelling of electrostatically deformed diaphragms." in *Proc. IEEE Micro Electro Mech. Syst. Conf.* (IEEE, New York, 1994), pp. 28-32.
14. T. Hochwitz, *private communication* (1995).

